Analysis of PLC Channels in Aircraft Environment and Optimization of some OFDM Parameters

Thomas Larhzaoui, Fabienne Nouvel, Jean-Yves Baudais
IETR
Rennes, France
thomas.larhzaoui@insa-rennes.fr, fabienne.nouvel@insa-rennes.fr, jean-yves.baudais@insa-rennes.fr

Virginie Degardin, Pierre Laly
IEMN
Lille, France
virginie.degardin@univ-lille1.fr, pierre.laly@univ-lille1.fr

Abstract— **PLC technology based on an OFDM communication scheme is considered for data transmission between a control unit and actuators located in an aircraft wing. In order to optimize some OFDM parameters, transfer function measurements have been performed on an avionic test bench. Based on experimental values of the coherence bandwidth and of the channel delay spread, it appears that the subcarrier spacing can be larger than the spacing specified in HomePlug AV, which usually applies for in-house environment. Similarly, the duration of the cyclic prefix can be reduced. This will allow meeting the real-time and determinism constraints of avionic systems.**

Keywords-PLC, OFDM, coherence bandwidth, dela spread, insertion gain, aircraft

I. INTRODUCTION

In future aircrafts, hydraulic flight control systems will be replaced by electric systems. The main interests are: a better reliability and flexibility, a decrease in maintenance costs, but the major problem is the increasing of wires length. In order to decrease this length, it has been proposed to use power line communications (PLC) technology for flight control systems. This technology has proven its reliability in in-home network with HomePlug AV (200 Mbit/s in the [1;30] MHz bandwidth [1]). In addition, there are numerous studies concerning PLC in different kinds of vehicles like cars [2], boats [3], and trains [4]. For aircrafts, [5] and [6] projects investigate the possibility of using PLC technology for the cabin light system.

In the near future, the AC power distribution will be replaced by a high voltage direct current (HVDC) distribution network. The authors in [7] studied the feasibility of using PLC technology between the power inverter and the actuator for flight control. In this paper, we focus on the PLC link on the HVDC network between a control unit and the power inverter feeding various active loads. Flight control systems do not require a high bit rate link, few Mbit/s being enough, but the communication must be highly reliable, deterministic, real time and must comply with the aeronautic standard DO-160 [8]. As shown in Fig. 1, we will consider the link between the control unit and the power inverter located near the actuators (spoilers) used for flight control. In this illustration, the PLC master (control unit side) transmits data to PLC slaves (power inverters side), corresponding to a point-to multipoint architecture. It is also possible to use point-to-point architecture, where one PLC node transmits data to another PLC node.

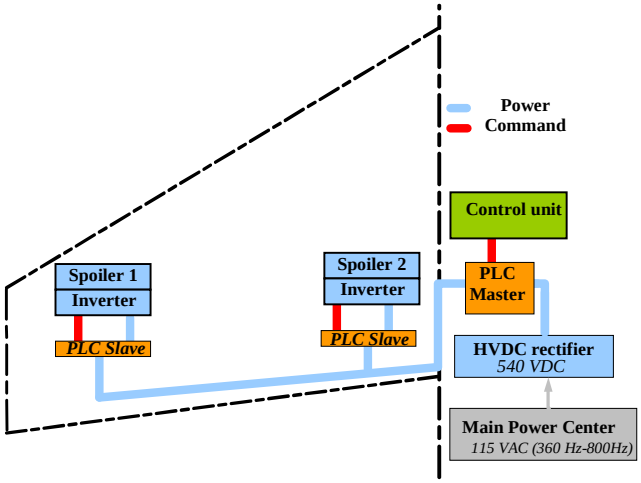

Figure 1. PLC system on aircraft wing

In order to transmit data over the HVDC network, we use either a capacitive coupler or an inductive coupler, the transmission being based on the usual Orthogonal Frequency Division Multiplexing (OFDM) transmission scheme. In addition, one of the major challenges of the command of the flight control systems is the real time constraints. Indeed, they operate at frequency about 1kHz (fast loop). According to the common practice, command systems must work six times quickly as much as the equipments that they command, which represent 6 kHz in our case. In addition, we must pay attention that there are several calculators in the loop, which require time processing. That's why we consider that our system do not exceed from 10 % to 20 % of the total time processing, which represent in our case from 17 µs to 34 µs. Thus, an analysis of the propagation channel made on a test bench representative of an actual configuration will allow the optimization of few OFDM parameters to show that is possible to have an OFDM duration in compliance with these real-time constraints.

This paper is organized as follows. In Section II, we describe the channel and the test bench, while results on the

 ISBN: 978-1-61208-305-6

insertion gain are presented in Section III. Section IV, describes the channel analysis and the optimization of the OFDM parameters is presented in Section V. A synthesis of the main results and a conclusion are given in Section VI.

II. DESCRIPTION OF THE TEST BENCH AND OF THE MEASUREMENT PROCEDURE

In this test bench, the channel is formed by a harness and at least 2 couplers.

A. *Configuration*

In this measurement campaign, two architectures were studied:

- The point-to-point architecture, with 2 couplers (Fig. 2 and Fig. 3)
- The point-to-multipoint architecture with 1 master and 2 slaves (Fig. 4)

The tests have been performed on a test bench whose active loads (540 V, 5 A) are representative of actual avionic loads and with a ± 270 DC power supply.

For this experimentation, the harness of 32 meters long, includes one twisted pair, one twisted quadrifilar cable, and one wire. The capacitive coupler transmits data between +270 V and -270 V DC, and is made by a transformer and two capacitors and use one twisted pair: signal is transmitted on one twisted pair between +270 V and -270 V.

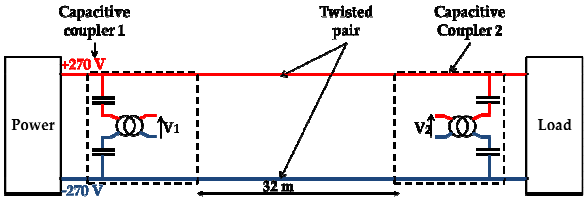

Figure 2. Point-to-point architecture with capacitive coupler

We have also considered another possibility, which is to use a twisted pair for the +270 V, rather than a single wire for the -270 V. In this case, the twisted pair is short circuited at both ends and an inductive coupler can be used as illustrated in Fig. 3: signal is transmitted on one twisted pair on +270 V. It must be emphasized that, for the same DC power, the diameter of each wire of the twisted pair can be reduced for avoiding an increase of the weight.

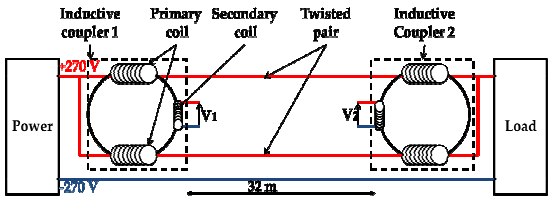

Figure 3. Point-to-point architecture with inductive coupler

In Fig. 4 we shows the last possibility: the point-to-multipoint architecture with inductive coupler. In this case we use three couplers on the +270 V. thus, harness is compose of one quadrifilar and one wire for the minus polarity. In the following, line 1 refers to the channel between coupler 1 and coupler 2 and line 2 to the channel between coupler 1 and coupler 3.

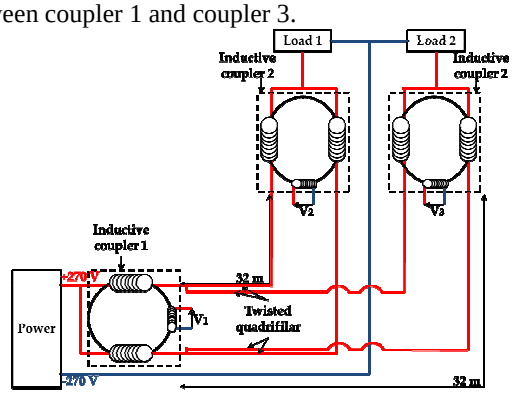

Figure 4. Point-to-multipoint architecture

B. *Measurements*

Measurements have been carried out with a network analyser in the [1;100] MHz bandwidth with a 5 kHz resolution bandwidth. For each configuration, the transfer functions were measured between the input/output V_1, V_2 and V_3.

III. INSERTION GAIN AND CHANNEL IMPULSE RESPONSE

Plots of Fig. 5 give the variation of the insertion gain (IG) versus frequency for the different architectures, while the cumulative distribution of IG is represented in Fig. 6. For the point-to-point configuration with an inductive coupler, IG first decreases linearly (in dB) with the frequency (up to 40 MHz), and varies from -5 to -25 dB. Then, IG remains nearly constant between 40 and 80 MHz and, beyond 80 MHz, decreases very rapidly. The other plots of Fig. 5 show that this behavior is nearly independent from the configuration except that we can note that the point-to-point link with a capacitive coupling presents several important fading in the low frequency band while at high frequency, (between 70 and 100 MHz), IG takes higher values than for the other configurations.

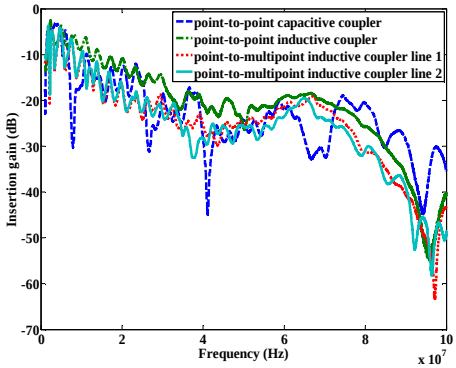

Figure 5. Insertion gains for the different configurations

In Fig. 6, probability at 10% is about -40 dB for inductive coupler and about -30 dB for capacitive coupler. The

probability at 50 % is about -20 dB for point-to-point architecture with inductive coupler and about -25 dB for the others configurations.

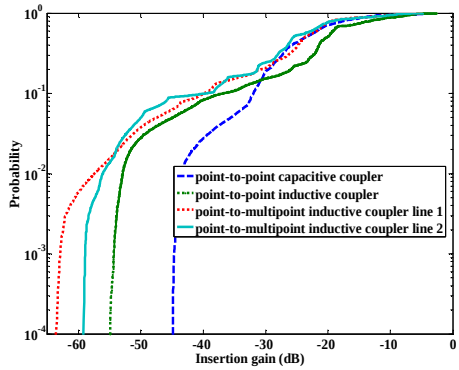

Figure 6. Cumulative distribution function of insertion gain

The channel impulse response has been deduced from the measurements of the complex transfer function by applying an inverse Fourier transform of 6000 points for [1;30] MHz and 20000 points for [1;100] MHz bandwidth. The results are shown in Fig. 7 and Fig. 8, by considering a frequency band either between 1 and 30 MHz or between 1 and 100 MHz.

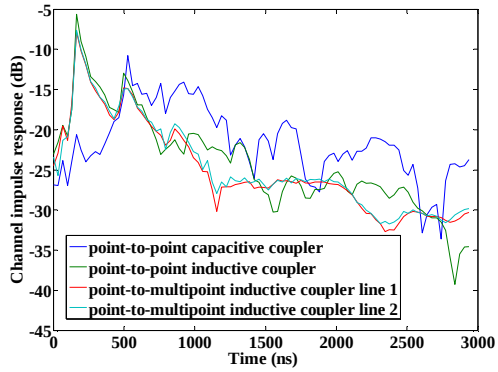

Figure 7. Channel impulse response in the [1;30] MHz

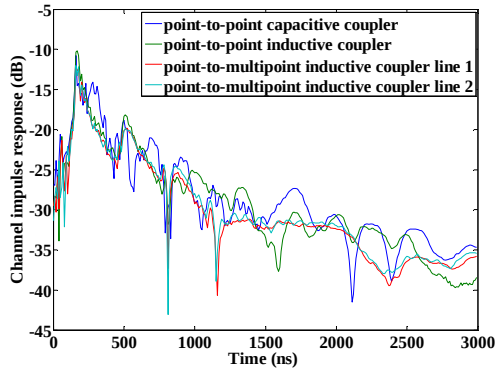

Figure 8. Channel impulse response in the [1-100] MHz

Coherence bandwidths and delay spreads are deduced from these results in frequency and time domain.

IV. COHERENCE BANDWIDTH AND DELAY SPREAD

The coherence bandwidth (CB) is deduced from the absolute value of the autocorrelation of the complex transfer function [9]. In the following, CB is calculated for a correlation coefficient of 0.9. Delay spread is calculated from the channel impulse responses according to [9]. Delay spread and coherence bandwidth are given in Table I, by considering either a 30 MHz or a 100 MHz transmission bandwidth.

It appears that the geometrical architecture and the type of coupler do not have a strong impact, the coherence bandwidth being of the order 700 – 1000 kHz, while the delay spread varies from 78 to 104 ns. These results are quite comparable to those obtained for other embedded systems as shown in Table II.

TABLE I. COHERENCE BANDWIDTH AND DELAY SPREAD FOR DIFFERENT CONFIGURATIONS

	Delay spread (ns)		**coherence bandwidth 0.9 (MHz)**	
Configurations	***[1;30] MHz***	***[1;100] MHz***	***[1;30] MHz***	***[1;100] MHz***
Capacitive coupler in point-to-point mode	*104*	*79*	*0,70*	*0,72*
Inductive coupler in point-to-point mode	*83*	*78*	*0,91*	*1,02*
Inductive coupler in point-to-multipoint mode (line 1)	*99*	*103*	*0,72*	*0,80*
Inductive coupler in point-to-multipoint mode (line 2)	*97*	*87*	*0,71*	*0,77*

TABLE II. COHERENCE BANDWIDTH AND DELAY SPREAD FOR DIFFERENT VEHICLES

References	**Bandwidth (MHz)**	**Delay spread (ns)**	**Coherence bandwidth (MHz)**
[2] car	[1-50]	[34-200]	[0.4-4.8]
[7] aircraft	[1-30]	100	[0,6-0,9]
[10] car	[0.3-100]	130	0.48
[11] car	[1-70]	380	[0.4-0.7]

V. OPTIMIZATION OF FEW OFDM PARAMETERS

A. *OFDM Subcarrier Spacing*

In order to meet the real time constraints, it is necessary to minimize the processing time of the data. Since fast Fourrier transform (FFT) is a time consuming process, one can try to decrease the number of carriers and choose, as in common practice, a carrier spacing equal to about 10% of the coherence bandwidth. Taking the values in Table I into

 ISBN: 978-1-61208-305-6

account, this leads to a 70 kHz subcarrier spacing, thus about three times the value given in HomePlug AV specifications (24.414 kHz). Furthermore, the baseband complex OFDM symbol will supply an I/Q RF modulator. This allows us to keep the FFT size equal to the number of carriers. In our case, the number of subcarriers is equal to 428 or 1428 for a transmission bandwidth of 30 MHz or 100 MHz, respectively.

B. *Interference Characterization*

Using the channel impulse response values, it is also possible to compute the Inter Symbol Interference (ISI) and the Inter Carrier Interference (ICI) in order to choose the optimal length L_{cp} of the cyclic prefix. A too long L_{cp} will reduce spectral efficiency and data rate. The power spectral density of (ISI) and (ICI) can be computed as follows [12]:

$$N_{ISI+ICI}(n) = 2\sigma_x^2 \sum_{l=L_{cp}+1}^{L_c-1} \left| \sum_{u=l}^{L_c-1} h(u) \exp\left(-j \frac{2\pi}{N} un \right) \right|^2 \quad (1)$$

In (1), σ_x^2 is the variance of modulated signal (and normalized to 1 W), h is the channel impulse response, L_c the channel length expressed in number of samples, L_{cp} being also expressed in terms of number of samples, N the number of carriers, and n the subcarrier index.

Fig. 9 and Fig. 10 give the interferences level, expressed in dBm/Hz for the inductive coupler in point-to-point configuration, and calculated in the [1;30] MHz and in the [1;100] MHz bandwidth, respectively. $N_{ISI+ICI}$ has been plotted versus the subcarrier number and for various lengths of the cyclic prefix (CP).

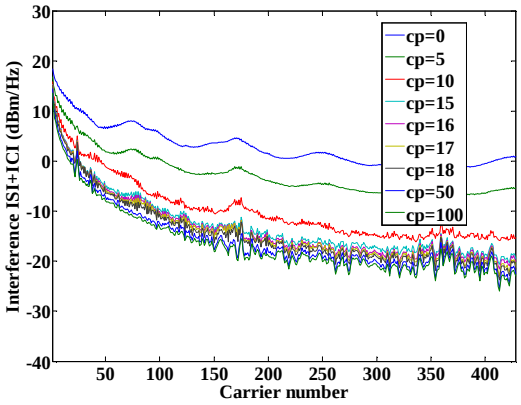

Figure 9. Interference in the [1-30] MHz bandwidth

As expected, the interference decreases rapidly with the length of the cyclic prefix but, beyond a given value, it does not vary appreciably.

From these curves, which have also been plotted for the other previously described network architectures, one can conclude that the CP length L_{cp} can be reduce at 15 samples (500 ns) for a 30 MHz band, and of 30 samples (300 ns) for a 100 MHz band.

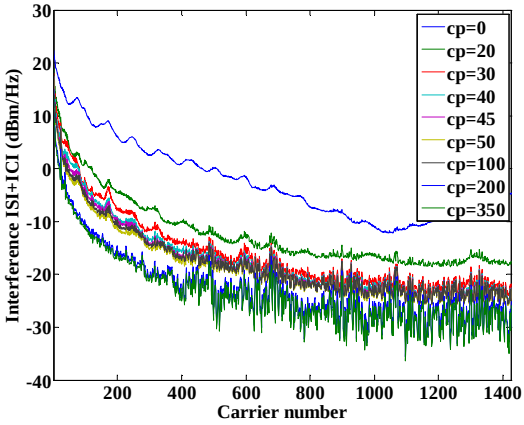

Figure 10. Interference in the [1-100] MHz bandwidth

As a comparison, if the cyclic duration was chosen equal to 2 to 4 times the delay spread, as suggested in [13], we would obtain a CP duration between 200 and 400 ns.

VI. SYNTHESIS AND CONCLUSION

For the aircraft environment studied in this paper, we have shown that it is possible to reduce the duration of an OFDM symbol compared to Homeplug Av standard, by increasing subcarrier spacing and decreasing the cyclic prefix duration. In the HomePlug AV standard the subcarrier spacing is 24.414 kHz, the minimum cyclic prefix duration is 5.56 µs, and the OFDM duration is 46.52 µs. In our application, we propose to increase the subcarrier spacing to 70 kHz and decrease the CP duration to 500 ns. Consequently, the symbol duration will be 14.78 µs instead of 46.52 µs (HPAV spec.). These results will help us to define the physical layer for a PLC avionics system in accordance with real-time constraints of a fast loop. This study can be applied to other critical avionic systems running on a HVDC network like landing gear. A fortiori, it is possible to use this study for a slow loop on HVDC network like, thrust reversal.

ACKNOWLEDGMENT

This paper is funded by Sagem and the harness was provided by Safran Engineering Services.

 ISBN: 978-1-61208-305-6

REFERENCES

[1] HomePlug Av specification, Version 1.1, May 21, 2007

[2] P. Tanguy and F. Nouvel, "In-vehicle PLC simulator based on channel measurements," International conference on intelligent transport system telecommunication (ITST),2010 , pp. 1-5.

[3] S. Barmada, L. Bellanti, M. Raugi, and M. Tucci, "Analysis of power-line communication, Channels in Ships," IEEE Trans. on Vehicular Technology, vol. 59, no. 7, september. 2010, pp. 3161-3170.

[4] S. Barmanda et al., "Design of a PLC system onboard trains: selection and analysis of the PLC channel," ISPLC, 2008, pp. 13-17.

[5] S. Bertuol et al, "Numerical Assessment of Propagation Channel Characteristics for Future Application of Power Line Communication in Aircraft," 10th Int. Symp. on EMC, September. 2011, pp. 506-511.

[6] V. Degardin, I. Junqua, M. Lienard, P. Degauque, and S. Bertuol, "Theoretical approach to the feasibility of power-line communication in aircrafts," IEEE Trans. VT, March. 2013, vol. 62, no. 3, pp. 1362-1366.

[7] K. Kilani, V. Degardin, P. Laly, M. Lienard, and P. Degauque, "Impulsive noise generated by a pulse width modulation inverter : modeling and impact on powerline communication," ISPLC, March. 2013, pp. 75-79.

[8] Do160,Environmental conditions and test procedures for airborne equipment, Standard, 2007.

[9] T.S. Rappaport, Wireless communication principle and practice, prentice hall patr,1996.

[10] A. B. Vallejo-Mora, J. J. Sanchez-Martínez, F. J. Cañete, C. J. Antonio, and L. Díez, "Characterization and evaluation of in-vehicle power line channels," in the IEEE Global Telecommunications Conference, 2010, pp. 1-5 , 2010.

[11] M. Lienard, M. Olivas Carrion, V. Degardin, and P. Degauque, "Modeling and analysis of in-vehicle power line communication Channels," IEEE transaction on vehicular technology, March. 2008 VOL. 57, NO. 2, pp. 670-679.

[12] W. Henkel, G. Taubock, P. Odling, P. Borjesson, and N. Petersson, "The cyclic prefix of ofdm/dmt - an analysis," in IEEE International Zurich Seminar on Broadband,Communications, 2002 pp. 22–1 –22–3.

[13] R. Van Nee and R. Prasad, "OFDM for wireless multimedia communications. Norwood," MA: Artech House, 2000.

 ISBN: 978-1-61208-305-6